GLRT Detector for Aspect-dependent Fluctuating Targets Using Distributed mmWave MIMO Radar Sensors

Ahmed Murtada*, Bhavani Shankar Mysore Rama Rao*, Udo Schroeder†
*Interdisciplinary Centre for Security, Reliability and Trust (SnT), University of Luxembourg
†IEE S.A., Luxembourg
{ahmed.murtada@uni.lu, bhavani.shankar@uni.lu, udo.schroeder@iee.lu}

***Abstract*—This paper addresses the problem of detecting fluctuating targets using distributed mmWave radar sensors designed for indoor monitoring scenarios. The proposed detector is derived based on the Generalized Likelihood Ratio Test (GLRT) aiming to estimate the fluctuation parameters of the targets at each sensor using multiple chirps. The resulting joint test is a weighted sum of individual tests applied to the square law detector output of each sensor. Weights are proportional to local Signal-to-Noise Ratios (SNR) at each sensor, which contrast extremely due to the variations in aspect angles and path losses for a single cell under test (CUT). Using Monte-Carlo simulations, we validate the performance of the proposed detector outperforming conventional detection methods that employ non-coherent integration of the chirps and aggregation of the tests for all sensors.**

***Index Terms*—Detection, GLRT, distributed MIMO Radars, fluctuating targets, aspect-dependent targets, indoor sensing.**

I. Introduction

The emergence of Multiple-Input Multiple-Output (MIMO) millimeter-wave (mmWave) radar sensors has received tremendous interest in recent years especially for indoor sensing applications [1]. Such applications include human detection and activity recognition [2], vital signs monitoring [3], and real-time tracking of multiple individuals [4], to name a few. Additionally, driven by the availability and affordability of such sensors, employing widely distributed sensing systems has drawn attention in the majority of applications due to the advantages that are allowed by such architectures [5]. In particular, the use of distributed sensors enables the capture of highly fluctuating and aspect angle-dependent targets. This results in a higher detection of such targets in addition to improving system robustness by providing redundancy in the events of occlusion or sensor failures [6]–[8].

Typically, detections by multiple widely distributed sensors are fused in the data domain after processing, rather than implementing a joint detection scheme. While data domain fusion allows for the use of simpler detection algorithms at each sensor, joint detection can potentially offer improved detection performance by appropriately weighting the data received from the different sensors and leveraging more the ones with a higher available signal-to-noise ratio (SNR) [9], [10]. Even though the optimum detector in the Neyman-Pearson sense for fluctuating targets observed with multistatic radars has long existed in the literature [11]–[13], to the best of the authors' knowledge, the corresponding sub-optimal Generalized Likelihood Ratio Test (GLRT) detector and the analysis of its performance versus the aspect angle dependence of the Radar Cross Section (RCS) have not been explicitly introduced, especially for indoor sensing environments. The optimum detector performs the Likelihood Ratio Test (LRT) assuming perfect knowledge of the expected average local SNRs available to each sensor which is impractical. Thus, an estimation of the average received power at each sensor is required for the implementation of the detector.

Accordingly, in this paper, we analytically devise the GLRT detector for fluctuating targets observed by widely distributed mmWave sensors each transmits multiple chips (pulses). Due to the angular diversity, the targets feature an aspect-dependent RCS that can vary significantly with respect to different sensors. We formulate the detection problem taking this into account and utilize Maximum Likelihood Estimation (MLE) in the derivation of the detector to achieve the optimum weighting in the GLRT sense. We evaluate the performance of the proposed detector using Monte-Carlo simulations and show that it outperforms the conventional detectors which employ non-coherent integration of multiple chirps and integrate the data from multiple sensors equally [14]. The proposed detector realizes higher gain in detection performance in the cases of higher variance of the RCS with respect to different sensors and achieves asymptotically the performance of the optimum LRT detector in extreme scenarios of RCS variation.

Throughout this paper, vectors are denoted in lowercase bold font, while matrices are in uppercase bold. $\mathbf{I}_L$ is the identity matrix of size $L \times L$ and $\mathbf{0}_N$ is a vector of all zeros of size $N \times 1$. The superscripts $.^T$ and $.^H$ denote, respectively, the transpose and the complex conjugate transpose of a vector or a matrix. The operators $|.|$ and $\|.\|_2$ are used for the matrix determinant and the Frobenius norm, respectively. The symbol $\otimes$ is used for the Kronecker product.

II. System and Signal Model

We consider a widely distributed radar system with Q mmWave MIMO radar sensors, each having N_{tx} and N_{rx}

This work is supported by Luxembourg National Research Fund (FNR) through the Industrial Fellowship grant IF/15364040/RADII.

transmitting and receiving antenna elements, respectively. Assume that $\mathbf{p}_q = [x_q, y_q, z_q]^T$ denotes the absolute position of the q^{th} radar sensor, where x_q, y_q, and z_q represents the absolute Cartesian coordinates, with $q = 1, 2, \ldots, Q$. In this case, a target with absolute position $\mathbf{p}_s = [x_s, y_s, z_s]^T$ and absolute velocity $\mathbf{v}_s = [v_{xs}, v_{ys}, v_{zs}]^T$, will have a relative distance R_q, azimuth θ_q, and elevation ϕ_q with the q^{th} radar sensor.

The target received signal can be expressed as

$$\mathbf{x}_q = \alpha_q \mathbf{s}_q(\theta_q, \phi_q) + \mathbf{w}_q \in \mathbb{C}^{N_{tx}N_{rx}\times 1} \tag{1}$$

where α_q indicates the complex value of the reflected signal at the q^{th} radar sensor which comprises path losses and target RCS, and fluctuates from pulse to pulse, $\mathbf{w}_q$ denotes the interference signal that can include both clutter and thermal noise. In this paper, we assume $\mathbf{w}_q \sim \mathcal{CN}(\mathbf{0}, \sigma_{\mathbf{w}}^2\mathbf{I})$ contains only receiver thermal noise which has a flat Power Spectral Density (PSD) with $P(f) = k_B T_0$, where k_B is the Boltzmann constant and T_0 is the effective noise temperature. Moreover, the signal steering vector is,

$$\mathbf{s}_q(\theta_q, \phi_q) = \mathbf{a}_q(\theta_q, \phi_q) \otimes \mathbf{b}_q(\theta_q, \phi_q),$$

where the spatial transmit and receive steering vectors are defined respectively as

$$\mathbf{a}_q(\theta, \phi) = \begin{bmatrix} e^{-j\mathbf{k}^T(\theta,\phi)\mathbf{p}_{q,1}} \\ e^{-j\mathbf{k}^T(\theta,\phi)\mathbf{p}_{q,2}} \\ \vdots \\ e^{-j\mathbf{k}^T(\theta,\phi)\mathbf{p}_{q,N_{tx}}} \end{bmatrix}, \mathbf{b}_q(\theta, \phi) = \begin{bmatrix} e^{-j\mathbf{k}^T(\theta,\phi)\mathbf{p}_{q,1}} \\ e^{-j\mathbf{k}^T(\theta,\phi)\mathbf{p}_{q,2}} \\ \vdots \\ e^{-j\mathbf{k}^T(\theta,\phi)\mathbf{p}_{q,N_{rx}}} \end{bmatrix},$$

and $\mathbf{k}(\theta, \phi) = \frac{2\pi}{\lambda}[\cos\theta\cos\phi, \sin\theta\cos\phi, \sin\phi]^T$ is the wavenumber vector with θ and ϕ are azimuth and elevation angles, respectively. $\mathbf{p}_{q,nt}$ and $\mathbf{p}_{q,nr}$ are the locations of the q^{th} radar transmit and receive array elements, respectively. At the fusion center, the received signals can be stacked by $\mathbf{x} = [\mathbf{x}_1^T, \mathbf{x}_2^T, ..., \mathbf{x}_Q^T]^T$ and $\mathbf{w} = [\mathbf{w}_1^T, \mathbf{w}_2^T, ..., \mathbf{w}_Q^T]^T$, and $\boldsymbol{\alpha} = [\alpha_1, \alpha_2, ..., \alpha_Q]^T$. By defining the steering matrix $\mathbf{S} \in \mathbb{C}^{QN_{tx}N_{rx}\times Q}$ as,

$$\mathbf{S} = \begin{bmatrix} \mathbf{s}_1(\theta_1, \phi_1) & \mathbf{0}_{N_{tx}N_{rx}} & \cdots & \mathbf{0}_{N_{tx}N_{rx}} \\ \mathbf{0}_{N_{tx}N_{rx}} & \mathbf{s}_2(\theta_2, \phi_2) & \cdots & \mathbf{0}_{N_{tx}N_{rx}} \\ \vdots & \vdots & \ddots & \vdots \\ \mathbf{0}_{N_{tx}N_{rx}} & \mathbf{0}_{N_{tx}N_{rx}} & \cdots & \mathbf{s}_Q(\theta_Q, \phi_Q) \end{bmatrix}.$$

The stacked received signal of M chirps (pulses) in one Coherent Processing Interval (CPI) reflected from a certain range CUT can be obtained by

$$\mathbf{X} = \mathbf{S}\boldsymbol{A} + \mathbf{W} \in \mathbb{C}^{\Omega\times M} \tag{2}$$

where the matrix $\mathbf{X} = [\mathbf{x}^{(1)}\mathbf{x}^{(2)}\cdots\mathbf{x}^{(M)}]$ collects the received signal of M chirps having the received signal at the m^{th} chirp obtained by

$$\mathbf{x}^{(m)} = \mathbf{S}\boldsymbol{\alpha}^{(m)} + \mathbf{w}^{(m)}, \tag{3}$$

$\boldsymbol{A} = [\boldsymbol{\alpha}^{(1)}, \boldsymbol{\alpha}^{(2)}, \cdots, \boldsymbol{\alpha}^{(M)}]$ represents the fluctuation of the amplitude of the signal from pulse to pulse, $\mathbf{W} = [\mathbf{w}^{(1)}, \mathbf{w}^{(2)}, \cdots, \mathbf{w}^{(M)}]$ is the aggregate matrix of thermal noise for all pulses, $\Omega = QN_{tx}N_{rx}$, and $m = 1, \cdots, M$.

The reflected signal amplitudes are assumed to be fluctuating from pulse to pulse at each sensor. We consider a Rayleigh fluctuation model (Swerling II) of the amplitudes of the reflected signals at the q^{th} sensor which is equivalent to its complex value being distributed as $\alpha_q \sim \mathcal{CN}(0, \sigma_{\alpha_q}^2)$.

Let $\mathcal{H}_0$ represent the null hypothesis that a target is absent, and $\mathcal{H}_1$ represent the alternative hypothesis that a target is present in the CUT. The detection problem can be cast as the following binary hypothesis test

$$\begin{cases} \mathcal{H}_0: & \mathbf{X} = \mathbf{W} \\ \mathcal{H}_1: & \mathbf{X} = \mathbf{S}\boldsymbol{A} + \mathbf{W} \end{cases} \tag{4}$$

In the next section, we provide the corresponding detector based on GLRT.

III. GLRT Detector Derivation

In order to derive the GLRT test, the probability density function (PDF) of the collection of the received signals from multiple chirps $\mathbf{X}$ under the null and the alternative hypotheses are to be evaluated. We first simplify the PDFs for a single chirp, then since the received signals from consecutive chirps are independent, the PDF of $\mathbf{X}$ is the multiplication of the PDFs of the single chirps. Under the null hypothesis, the received signal contains only the noise that is modeled as a central complex white Gaussian noise and has the PDF

$$p(\mathbf{x} \mid \mathcal{H}_0) = \frac{1}{\sqrt{\pi^{2\Omega}\left|\mathbf{C}_{\mathbf{ww}}\right|}} \exp\left(-\frac{1}{2}\mathbf{x}^H\mathbf{C}_{\mathbf{ww}}^{-1}\mathbf{x}\right) \tag{5}$$

where $\mathbf{C}_{\mathbf{ww}} = \sigma_{\mathbf{w}}^2\mathbf{I}_\Omega$. Similarly, under the alternative hypothesis, the received signal has the PDF

$$p(\mathbf{x} \mid \mathcal{H}_1) = \frac{1}{\sqrt{\pi^{2\Omega}\left|\mathbf{C}_{\mathbf{xx}}\right|}} \exp\left(-\frac{1}{2}\mathbf{x}^H\mathbf{C}_{\mathbf{xx}}^{-1}\mathbf{x}\right) \tag{6}$$

where in this case, from (3), the covariance matrix of the received signal is $\mathbf{C}_{\mathbf{xx}} = \mathbf{S}\mathbf{C}_{\alpha\alpha}\mathbf{S}^H + \mathbf{C}_{\mathbf{ww}}$ since $\boldsymbol{\alpha}$ and $\mathbf{w}$ are independent, where $\mathbf{C}_{\alpha\alpha}$ is the covariance matrix of $\boldsymbol{\alpha}$.

Since the reflectivity coefficients with respect to each sensor are mutually independent, the covariance matrix $\mathbf{C}_{\boldsymbol{\alpha}\boldsymbol{\alpha}}$ takes the form $\mathbf{C}_{\alpha\alpha} = \operatorname{diag}\left(\sigma_{\alpha_1}^2, \sigma_{\alpha_2}^2, \ldots, \sigma_{\alpha_Q}^2\right)$ which leads to a block diagonal structure of the covariance matrix $\mathbf{C}_{\mathbf{xx}}$ with the q^{th} block that has the dimensions $\zeta \times \zeta$ defined as

$$[\mathbf{C}_{\mathbf{xx}}]_q = \sigma_{\alpha_q}^2\mathbf{s}_q\mathbf{s}_q^H + \sigma_{\mathbf{w}}^2\mathbf{I}_\zeta \tag{7}$$

Under the alternative hypothesis (6), the log-likelihood function is

$$\mathcal{L}\left(p\left(\mathbf{x} \mid \mathcal{H}_1\right)\right) = -2\ln(\pi) - \frac{1}{2}\ln\left|\mathbf{C}_{\mathbf{xx}}\right| - \frac{1}{2}\mathbf{x}^H\mathbf{C}_{\mathbf{xx}}^{-1}\mathbf{x} \tag{8}$$

where the quadratic term of the likelihood function is written and simplified using the Matrix inversion lemma as,

$$\begin{aligned} \mathbf{x}^H\mathbf{C}_{\mathbf{xx}}^{-1}\mathbf{x} &= \sum_{q=1}^{Q}\mathbf{x}_q^H\left(\sigma_{\alpha_q}^2\mathbf{s}_q\mathbf{s}_q^H + \sigma_{\mathbf{w}}^2\mathbf{I}_\zeta\right)^{-1}\mathbf{x}_q \\ &= \sum_{q=1}^{Q}\mathbf{x}_q^H\left(\frac{1}{\sigma_{\mathbf{w}}^2}\mathbf{I}_\zeta - \frac{\sigma_{\alpha_q}^2/\sigma_{\mathbf{w}}^2}{\sigma_{\mathbf{w}}^2 + \zeta\sigma_{\alpha_q}^2}\mathbf{s}_q\mathbf{s}_q^H\right)\mathbf{x}_q. \end{aligned} \tag{9}$$

Similarly, using the Matrix determinant lemma, the logarithmic term can be written as

$$\begin{aligned}\ln|\mathbf{C_{xx}}| &= \ln\left(\prod_{q=1}^{Q}\left|\sigma^2_{\alpha_q}\mathbf{s}_q\mathbf{s}_q^H+\sigma^2_{\mathbf{w}}\mathbf{I}_\zeta\right|\right)\\ &= \sum_{q=1}^{Q}\ln\left(\left|\sigma^2_{\alpha_q}\mathbf{s}_q\mathbf{s}_q^H+\sigma^2_{\mathbf{w}}\mathbf{I}_\zeta\right|\right)\\ &= \ln|\mathbf{C_{ww}}|+\sum_{q=1}^{Q}\ln\left(1+\zeta\frac{\sigma^2_{\alpha_q^2}}{\sigma^2_{\mathbf{w}}}\right).\end{aligned} \tag{10}$$

Accordingly, considering the binary hypothesis test in (4), the optimum detector based on GLRT is obtained by

$$t_{\text{GLRT}}=\ln\left\{\frac{\max\limits_{\sigma^2_{\alpha_1},\sigma^2_{\alpha_2},\cdots,\sigma^2_{\alpha_Q}}\prod_{m=1}^{M}\left(p(\mathbf{x}^{(m)}\mid\mathcal{H}_1)\right)}{\prod_{m=1}^{M}p(\mathbf{x}^{(m)}\mid\mathcal{H}_0)}\right\}\underset{\mathcal{H}_0}{\overset{\mathcal{H}_1}{\gtrless}}\eta \tag{11}$$

Using (9) and (10), the GLRT in (11) can be expanded in terms of the received signal of all chirps and sensors as

$$\begin{aligned}t_{\text{GLRT}} &= \sum_{m=1}^{M}\left\{\begin{array}{c}\mathbf{x}^{(m)^H}\left(\mathbf{C}_{\mathbf{w}}^{-1}-\hat{\mathbf{C}}_{\mathbf{xx}}^{-1}\right)\mathbf{x}^{(m)}\\ +\ln|\mathbf{C_{ww}}|-\ln\left|\hat{\mathbf{C}}_{\mathbf{xx}}\right|\end{array}\right\}\underset{\mathcal{H}_0}{\overset{\mathcal{H}_1}{\gtrless}}2\eta\\ &= \sum_{m=1}^{M}\left\{\begin{array}{c}\sum_{q=1}^{Q}\mathbf{x}_q^{(m)^H}\left(\frac{\hat{\sigma}^2_{\alpha_q}/\sigma^2_{\mathbf{w}}}{\sigma^2_{\mathbf{w}}+\zeta\hat{\sigma}^2_{\alpha_q}}\mathbf{s}_q\mathbf{s}_q^H\right)\mathbf{x}_q^{(m)}\\ -\sum_{q=1}^{Q}\ln\left(1+\zeta\frac{\hat{\sigma}^2_{\alpha_q^2}}{\sigma^2_{\mathbf{w}}}\right)\end{array}\right\}\underset{\mathcal{H}_0}{\overset{\mathcal{H}_1}{\gtrless}}2\eta\\ &= \sum_{m=1}^{M}\left\{\begin{array}{c}\sum_{q=1}^{Q}\left(\frac{\hat{\sigma}^2_{\alpha_q}/\sigma^2_{\mathbf{w}}}{\sigma^2_{\mathbf{w}}+\zeta\hat{\sigma}^2_{\alpha_q}}\right)\left\|\mathbf{s}_q^H\mathbf{x}_q^{(m)}\right\|_2^2\\ -\sum_{q=1}^{Q}\ln\left(1+\zeta\frac{\hat{\sigma}^2_{\alpha_q^2}}{\sigma^2_{\mathbf{w}}}\right)\end{array}\right\}\underset{\mathcal{H}_0}{\overset{\mathcal{H}_1}{\gtrless}}2\eta\end{aligned} \tag{12}$$

where $\hat{\mathbf{C}}_{\mathbf{xx}}$ is the estimated covariance matrix constructed by the estimated values of $\hat{\sigma}^2_{\alpha_q}$ through Maximum Likelihood Estimation (MLE) by minimizing the negative likelihood $-\mathcal{L}\left(\prod_{m=1}^{M}\left(p\left(\mathbf{x}^{(m)}\mid\mathcal{H}_1\right)\right)\right.$ with respect to $\sigma^2_{\alpha_q}$. Note that this minimization can be done separately for each $\sigma^2_{\alpha_q}$ since they are independent. More specifically,

$$\begin{aligned}\hat{\sigma}^2_{\alpha_q} &= \min_{\sigma^2_{\alpha_q}}\left\{-\mathcal{L}\left(\prod_{m=1}^{M}p\left(\mathbf{x}^{(m)}\mid\mathcal{H}_1\right)\right)\right\}\\ &= \min_{\sigma^2_{\alpha_q}}\left\{\begin{array}{c}\sum_{m=1}^{M}\mathbf{x}_q^{(m)^H}\left(\frac{\sigma^2_{\alpha_q}/\sigma^2_{\mathbf{w}}}{\sigma^2_{\mathbf{w}}+\zeta\sigma^2_{\alpha_q}}\mathbf{s}_q\mathbf{s}_q^H\right)\mathbf{x}_q^{(m)}\\ -\ln\left(1+\zeta\frac{\sigma^2_{\alpha_q}}{\sigma^2_{\mathbf{w}}}\right)\end{array}\right\}\end{aligned} \tag{13}$$

Solving for $\sigma^2_{\alpha_q}$, yields the solution

$$\hat{\sigma}^2_{\alpha_q}=\frac{\frac{1}{M}\sum_{m=1}^{M}\left\|\mathbf{s}_q^H\mathbf{x}_q^{(m)}\right\|_2^2-\zeta\sigma^2_{\mathbf{w}}}{\zeta^2} \tag{14}$$

which is the estimation of signal power at the q^{th} sensor. The MLE estimate above requires knowledge of the noise power that is estimated using secondary data in adjacent cells free of a target $\mathbf{X}_{sec}$ as $\sigma^2_{\mathbf{w}}=\text{tr}\left[\frac{1}{M}\sum_{m=1}^{M}\mathbf{X}_{sec}\mathbf{X}_{sec}^H\right]/\Omega$.

It is noted from (12) that the GRLT test is a weighted sum of the square output of the matched filter of different sensors where the weights are proportional to the local SNRs available at the sensors, as suggested in the literature. In the sequel, the performance of the proposed detector is analyzed numerically.

IV. Numerical Analysis

In this section, we evaluate the proposed GLRT detector numerically using Monte-Carlo simulations. The detector's performance is demonstrated through the use of Receiver Operating Characteristics (ROC) curves. Our proposed detector is compared to the conventional detector for fluctuating targets, which comprises square-law detectors at each sensor, with their output being non-coherently integrated [14]. Throughout this section, we consider distributed sensors, each equipped with $N_{tx}=2$ transmitting antennas and $N_{rx}=3$ receiving antennas for the different configurations and scenarios considered. We also considered the RF parameters of the sensors that match the operating parameters for TI IWR6843ISK radar [15].

First, in Fig. 1, with $Q=4$ sensors, an average post-processing $\text{SNR}_{\text{post}}=13$ dB, and $M=3Q$ chirps, we show the performance of the GLRT detector for three cases of variance in aspect angle dependence of the fluctuating targets. In addition to the ROC of the conventional detector, we show the ROC of the optimum LRT detector for multistatic radars [11] which assumes perfect knowledge of the local SNRs at each sensor. The target in Fig. 1(a) is assumed to be fluctuating with the same average power $\sigma_{\alpha_q^2}$ with respect to all sensors (isotropic). Accordingly, as expected, all three detectors manifest the same performance since the optimum test weights the output of the matched filters of each sensor equally which is equivalent to the conventional detector that applies no weighting. On the other hand, in Fig. 1(b) and Fig. 1(c), the RCS is assumed aspect-dependent with its value varying in a range of 10 dB and 20 dB, respectively. The depicted performance suggests that the proposed detector is crucial when RCS varies dramatically with aspect angle. Moreover, Fig. 1(c) shows that the proposed detector may achieve asymptotically the performance of the optimum detector which assumes perfect knowledge of local SNRs in extreme cases of RCS aspect variance. We also included the detection performance of individual sensors with no fusion; in the figure, this is clearly inferior since the total SNR comes from the integration of all sensors.

Fig. 2 illustrates the performance of the proposed detector versus the number of distributed sensors while keeping the post-processing SNR identical, and the number of integrated chirps $M=3Q$. Needless to mention, the proposed detector does not bring any gain in performance with respect to the conventional one in the case of $Q=1$ since no angle diversity is exploited. Likewise, it can be also anticipated that the larger

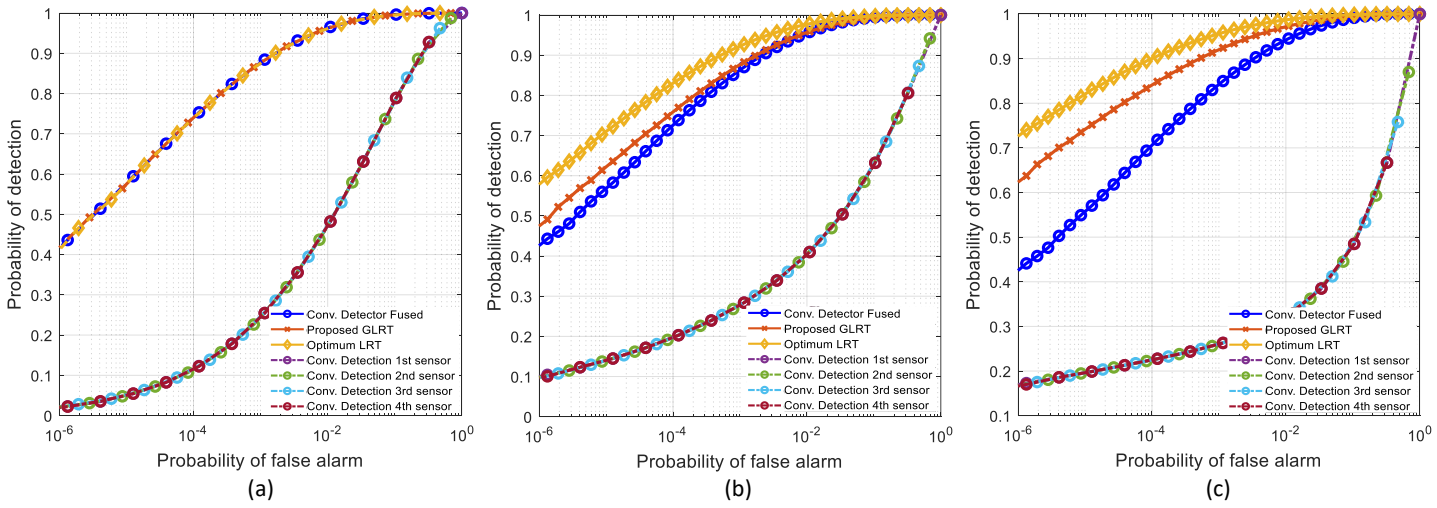

Fig. 1. ROC curves for the proposed GLRT detector compared with conventional and optimum LRT detectors where $Q = 4$, $M = 3Q$, $\text{SNR}_{post} = 13$ dB for a fluctuating target with (a) isotropic RCS, (b) Aspect-dependent RCS with maximum variation 10 dB, (c) Aspect-dependent RCS with maximum variation 20 dB.

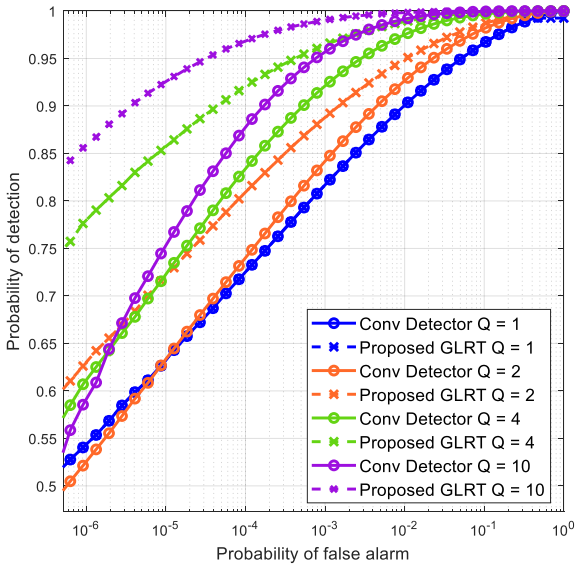

Fig. 2. ROC curves of the proposed GLRT detector versus the number of distributed sensors, $\text{SNR}_{post} = 13$ dB, $M = 3Q$.

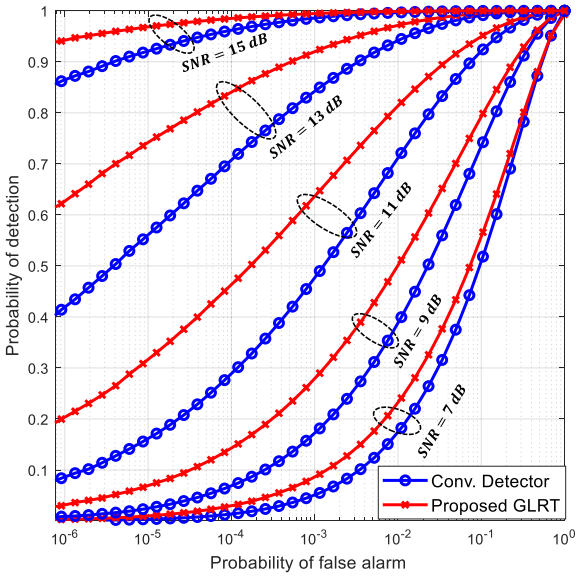

Fig. 3. ROC curves of the proposed GLRT detector versus different values of post-processing SNR, $Q = 4$, $M = 3Q$

the number of sensors, the higher gain is obtained by the proposed detector relying on more measurements with high average power and weighing the unfavorable ones less.

Similarly, the performance of the detector versus different values of SNR_{post} and different number of chirps M while keeping $Q = 4$ is depicted in Fig. 3 and Fig. 4, respectively. It can be observed that the proposed detector provides the highest gain in the mid-range of SNR values. This can be attributed to the fact that, at very low SNR values, most of the received signals from different sensors are inadequate for detection. Also, for very high SNR values, all the received signals from different sensors can be highly reliable for detection. This makes weighting in both cases of high and low SNR not bringing excessive gain in performance. On the other hand, increasing the number of chirps enhances the estimation of the received signal power in each sensor which leads to better performance of the proposed detector. Note that as seen in Fig. 4, a few chirps as low as the number of sensors is sufficient to realize a performance gain with the proposed detector.

V. Conclusion

In this paper, we derived a GLRT detector for aspect-dependent fluctuating targets observed by widely distributed MIMO radar sensors transmitting multiple chirps. Using the received signal of multiple chirps, the average received signal

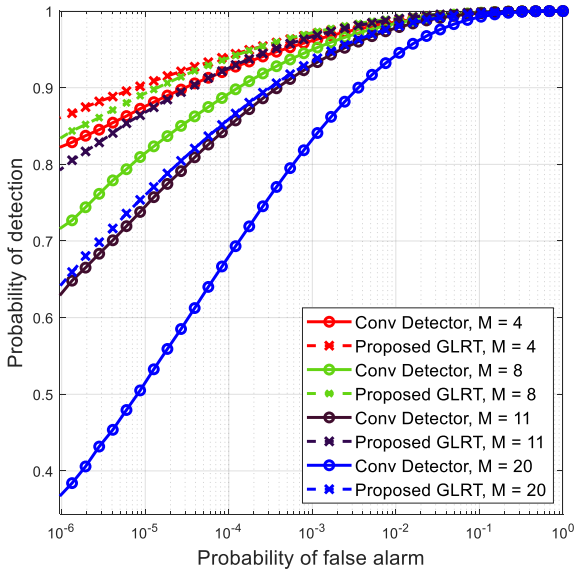

Fig. 4. ROC curves of the proposed GLRT detector versus the number of integrated chirps, $\text{SNR}_{post} = 13$ dB, $Q = 4$

power at each sensor is estimated through MLE and plugged into the likelihood ratio test to achieve the GLRT detector. The resulting detector is a weighted sum of the individual tests at each sensor, where the weights are proportional to the local SNR values that vary significantly due to the variance in RCS versus different aspect angles in addition to the different path losses towards each sensor. We demonstrated the performance of the devised detector through Monte-Carlo simulations and showed that it outperforms the conventional detector by employing non-coherent integration of the chirps and equal aggregation of the tests performed on each sensor's received signal. The numerical simulations show that in the cases where the RCS of the targets contrast significantly, the proposed detector asymptotically achieves the optimum detector's performance with perfect knowledge of local SNR values. Additionally, the simulations offer insights into the performance of the proposed detector versus post-processing SNR, the number of distributed sensors, and the number of integrated chirps.

REFERENCES

[1] G. Gennarelli, F. Soldovieri, and M. Amin, "Radar for indoor surveillance: state of art and perspectives," in *Multimodal Sensing: Technologies and Applications*, vol. 11059. SPIE, Jun. 2019, p. 1105903.

[2] Y. Kim and T. Moon, "Human Detection and Activity Classification Based on Micro-Doppler Signatures Using Deep Convolutional Neural Networks," *IEEE Geoscience and Remote Sensing Letters*, vol. 13, no. 1, pp. 8–12, Jan. 2016.

[3] G. Beltrão, R. Stutz, F. Hornberger, W. A. Martins, D. Tatarinov, M. Alaee-Kerahroodi, U. Lindner, L. Stock, E. Kaiser, S. Goedicke-Fritz, U. Schroeder, B. S. M. R., and M. Zemlin, "Contactless radar-based breathing monitoring of premature infants in the neonatal intensive care unit," *Scientific Reports*, vol. 12, no. 1, p. 5150, Mar. 2022.

[4] H. Cui and N. Dahnoun, "High Precision Human Detection and Tracking Using Millimeter-Wave Radars," *IEEE Aerospace and Electronic Systems Magazine*, vol. 36, no. 1, pp. 22–32, Jan. 2021.

[5] A. M. Haimovich, R. S. Blum, and L. J. Cimini, "MIMO Radar with Widely Separated Antennas," *IEEE Signal Processing Magazine*, vol. 25, no. 1, pp. 116–129, 2008.

[6] E. Fishler, A. Haimovich, R. Blum, L. Cimini, D. Chizhik, and R. Valenzuela, "Spatial Diversity in Radars—Models and Detection Performance," *IEEE Transactions on Signal Processing*, vol. 54, no. 3, pp. 823–838, Mar. 2006.

[7] T. Aittomaki and V. Koivunen, "Performance of MIMO Radar With Angular Diversity Under Swerling Scattering Models," *IEEE Journal of Selected Topics in Signal Processing*, vol. 4, no. 1, pp. 101–114, Feb. 2010.

[8] V. Chernyak, "Multisite radar systems composed of MIMO radars," *IEEE Aerospace and Electronic Systems Magazine*, vol. 29, no. 12, pp. 28–37, Dec. 2014.

[9] P. K. Varshney, *Distributed Detection and Data Fusion*. New York, NY: Springer New York, 1997.

[10] B. K. Chalise, D. M. Wong, M. G. Amin, A. F. Martone, and B. H. Kirk, "Detection, mode selection, and parameter estimation in distributed radar networks : Algorithms and implementation challenges," *IEEE Aerospace and Electronic Systems Magazine*, pp. 1–16, 2022.

[11] E. D'Addio, A. Farina, E. Conte, and M. Longo, "Multistatic Detection of Radar Signals for Swerling Models of the Target," 1985.

[12] E. D'Addio and A. Farina, "Overview of detection theory in multistatic radar," 1986.

[13] V. Aloisio, "Optimum detection of moderately fluctuating radar targets," *IEE Proceedings - Radar, Sonar and Navigation*, vol. 141, no. 3, p. 164, 1994.

[14] J. V. DiFranco and W. L. Rubin, *Radar Detection*. Raleigh, NC: SciTech Publishing, Apr. 2004.

[15] "IWR6843 data sheet, product information and support | TI.com."